

Formation of an Fe(III)-Tyrosinate Complex During Biomineralization of H-Subunit Ferritin

Geoffrey S. Waldo, Jinshu Ling, Joann Sanders-Loehr, Elizabeth C. Theil*

An iron(III)-tyrosinate complex was identified in ferritin by ultraviolet-visible and resonance Raman spectroscopies. Previously, a specific amino acid side chain coordinated to iron in ferritin was not known. Ferritin protein was overexpressed in *Escherichia coli* from complementary DNA sequences of bullfrog red cell ferritin. The purple iron(III)-tyrosinate intermediate that formed during the first stages of iron uptake was replaced by the amber multinuclear iron(III)-oxo complexes of fully mineralized ferritin. Only the H subunit formed detectable amounts of the iron(III)-tyrosinate complex, which may explain the faster rates of iron biomineralization in H- compared to L-type ferritin.

Ferritin, a large, hollow protein encasing a mineral core of hydrated ferric oxide or ferric phosphate, contains up to 4500 Fe atoms for use in such reactions as DNA synthesis, respiration, photosynthesis, and nitrogen fixation (1, 2). The spherical apoprotein is composed of 24 polypeptide subunits associated by noncovalent interactions. High conservation of amino acid sequence in ferritin from prokaryotes (3), plants, and animals suggests an ancient progenitor form of ferritin (1, 2, 4). Two ferritin subunits, H and L, occur in vertebrates (1, 2).

Specific Fe-amino acid complexes have not been identified in ferritin. Extended x-ray absorption fine structure and Mössbauer spectroscopies have shown Fe(III) bound to oxygen or nitrogen ligands in mononuclear and multinuclear forms (5, 6). N-vanadium complexes have been demonstrated (7). In ferritin, terbium (Tb) bound to Glu, Asp, and His has been observed by x-ray diffraction; the site influences the rate of biomineralization (8).

Bullfrog red cell H and L ferritins, overexpressed in *Escherichia coli* (9) (Fig. 1A), displayed the relative rates of polynuclear Fe-complex formation typical for vertebrate H and L ferritins; polynuclear Fe-complex formation is far more rapid in the H-subunit class than in that of the L (10, 11) (Fig. 1B). Two residues, Glu⁵⁸ and His⁶¹ (Fig. 2), have been shown by site-directed mutagenesis to be required for rapid polynuclear Fe-complex formation (ferroxidation) in human H-subunit ferritin (8). Bullfrog red cell L ferritin also contains the Glu⁵⁸ and His⁶¹ residues (Fig. 2). Nevertheless, the bullfrog red cell L ferritin does not display the rapid color formation associated with H-subunit ferritins (Fig. 1B). Thus, addi-

tional structural differences between H- and L-type ferritin subunits, previously unappreciated, may contribute to the observed variations in function during Fe uptake.

We identified a purple Fe(III)-tyrosinate [Fe(III)-Tyr] complex early in the biomineralization of H-type ferritin. The distinctive purple complex formed within seconds when Fe(II) was added to bullfrog H-subunit ferritin (0.5 mM in subunits) at low Fe loadings (≤ 48 Fe atoms per molecule) in the presence of air. Within 5 min, at 48 Fe atoms per molecule, the purple color was replaced by the amber color of mineralized ferritin. Under identical conditions, only the amber color developed in bullfrog L-subunit fer-

ritin, and it formed at a reduced rate. The formation of the H subunit-specific purple species was dioxygen-dependent. After the admission of air to anaerobic solutions of H-subunit ferritin (1 mM in subunits) and Fe(II) (24 Fe atoms per molecule), color formation at 420 nm was biphasic (Fig. 3A). The 550-nm absorption was maximal at 6 min and then slowly decreased.

The purple Fe-ferritin complex gave a rich Raman spectrum upon excitation within the 550-nm absorption band (Fig. 3B). On the basis of model studies and comparisons to previously reported Raman data of other Fe-Tyr complexes (12, 13), the principal Fe(III)-phenolate Raman modes may be identified in the Fe-apoferritin Raman spectrum (Fig. 3B and Table 1). Raman spectra obtained at a series of excitation energies within the 550-nm absorption envelope indicate that the intensities of the Fe-tyrosinate modes track the 550-nm absorption band. This provides strong evidence that the 550-nm peak in the Fe-ferritin complex arises from a Tyr \rightarrow Fe(III) charge transfer band.

Heterogeneity was observed in the Fe(III)-phenolate ν_{C-O} region of the Raman spectrum of H-subunit ferritin (1288 and 1300 cm^{-1} , Fig. 3B). The splitting and relative intensities of the peaks were both constant for different samples. The frequency of the ν_{C-O} mode is more sensitive to the Tyr environment than that of either the ν_{C-C} or δ_{C-H} mode (Table 1). Two ν_{C-O}

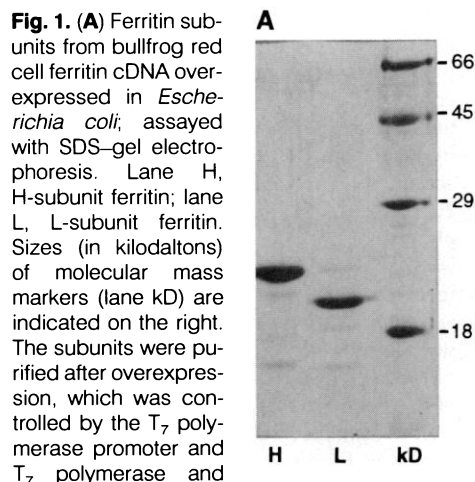
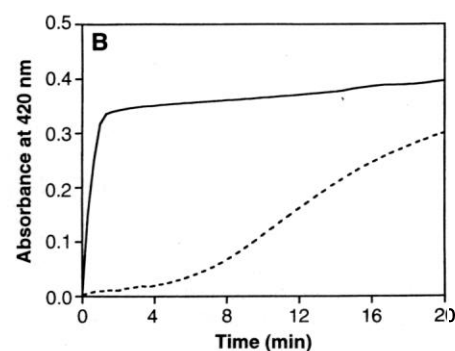


Fig. 1. (A) Ferritin subunits from bullfrog red cell ferritin cDNA overexpressed in *Escherichia coli*; assayed with SDS-gel electrophoresis. Lane H, H-subunit ferritin; lane L, L-subunit ferritin. Sizes (in kilodaltons) of molecular mass markers (lane kD) are indicated on the right. The subunits were purified after overexpression, which was controlled by the T₇ polymerase promoter and T₇ polymerase and regulated by the Lac operator in *E. coli* BL21 (DE3) + pLysS (H subunit) or BL21 (DE3) (L subunit) (22). The sequences PJD5F12 (H subunit) and PJD1D8 (L subunit) (9) were inserted in the Nde I site of a PET 3 vector; translation initiation began at the natural start sites of the ferritin sequences. Ferritin was recovered from the supernatant fraction of sonicated extracts after heating (70°C for 15 min), centrifugation, precipitation from the supernatant by 80% NH₄SO₄, and anion-exchange chromatography on a Mono Q column (Pharmacia). Gel filtration showed that both H- and L-ferritin subunits assembled as homopolymers into 24 mers of the natural size. The average yield of purified ferritin was ~30 mg from 3 g of cell pellet (1 liter of cell culture). **(B)** Ultraviolet-visible spectroscopy of bullfrog red cell ferritins during amber color formation (change in absorbance at 420 nm). Subunits of H ferritin (—) exhibited much faster kinetics of color formation than those of L ferritin (- - -). Fe(II) was added as a freshly prepared solution of Fe(II)SO₄ to H- or L-ferritin samples in 1-ml quartz cuvettes. Reactions were performed at an ambient temperature of 25°C with proteins in an air-saturated MOPS buffer, pH = 7.0, containing 0.45 M Cl⁻; the Fe-to-protein ratio was 480, and the initial Fe(II) concentration was 0.5 mM. The results are representative of two samples.



G. S. Waldo and E. C. Theil, Departments of Biochemistry and Physics, North Carolina State University, Raleigh, NC 27695.

J. Ling and J. Sanders-Loehr, Department of Chemical and Biological Sciences, Oregon Graduate Institute, Beaverton, OR 97006.

*To whom correspondence should be addressed.

stretches suggest that the peaks are associated with two different Fe(III)-Tyr moieties. Amino acid sequence data for several ferritins (Fig. 2) reveal three conserved Tyr side chains (positions 25, 28, and 30). Both Tyr²⁸ and Tyr³⁰ are conserved in all H and L vertebrate ferritins. Only Tyr²⁵ is H subunit-specific, suggesting that Tyr²⁵ could be required for the formation of the Fe(III)-Tyr complex. This residue appears to be positioned near the surface of the ferritin protein coat (14) and may be the

Table 1. Characteristic Raman frequencies (in cm⁻¹) for ferric phenolates. Sources of data: Fe(SALEN) (OC₆H₄-4-CH₃) (32); beef spleen purple acid phosphatase (31); catechol 1,2-dioxygenase (12); protocatechuate 3,4-dioxygenase (12); ferritin intermediate, this report. SALEN = 1,2 bis(salicylideneiminato) ethane.

Ferric phenolate	$\nu_{\text{Fe-O}}$	$\delta_{\text{C-H}}$	$\nu_{\text{C-O}}$	$\nu_{\text{C-C}}$	$\nu_{\text{C-C}}$
Fe(SALEN) (OC ₆ H ₄ -4-CH ₃)	568	1168	1272	1501	1603
Purple acid phosphatase	575	1164	1281	1497	1597
Catechol 1,2-dioxygenase		1175	1289	1506	1604
Protocatechuate 3,4-dioxygenase		1176	1265	1505	1605
Ferritin intermediate	589	1167	1288	1502	1602
			1300		

Fig. 2. The H-subunit-specific Tyr and Tb (ferroxidase) ligands with partial amino acid sequences for several ferritins. Boxes: a, residues explicitly shown by site-directed mutagenesis to be required for ferroxidation activity by human H-subunit ferritin; b, Tyr conserved in all vertebrate ferritins; c, Tyr specific to H-subunit ferritins. Rows: 1, horse spleen L subunit (23); 2, human liver L subunit (24); 3, rat liver L subunit (25); 4, rabbit liver L subunit (26); 5, tadpole red cell L subunit (9); 6, human liver H subunit (24); 7, rat liver H subunit (27); 8, chicken red cell H subunit (28); and 9, tadpole red cell H subunit (9). Numbering of ferritin subunit sequences is based on the horse spleen L subunit. Abbreviations for amino acids are as in (29).

		25	30	55	60
1	HoSp L	R A S	Y T Y	L S L G F	A E E K R E G
2	HuLi L	Q A S	Y T Y	L S L G F	A E E K R E G
3	RaLi L	R A S	Y T Y	L S L G F	A E E K R E G
4	RbLi L	L R A S	Y T Y	L S L G F	A E E K R E A
5	TdRC L	H S S	Y V Y	L S M A S	S E E E K E H
6	HuLi H	Y A S	Y V Y	L S M S Y	S H E E R E H
7	RaLi H	Y A S	Y V Y	L S M S C	S H E E R E H
8	ChRC H	Y A S	Y V Y	L S M S Y	S H E E R E H
9	TdRC H	Y A S	Y T Y	L S M A F	S H E E R E H

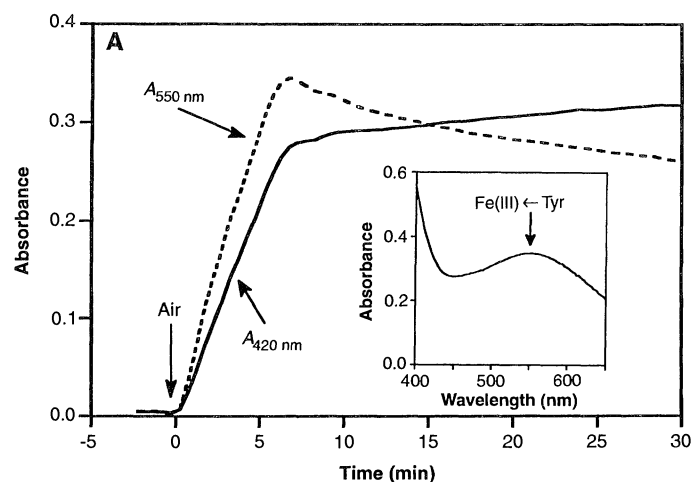
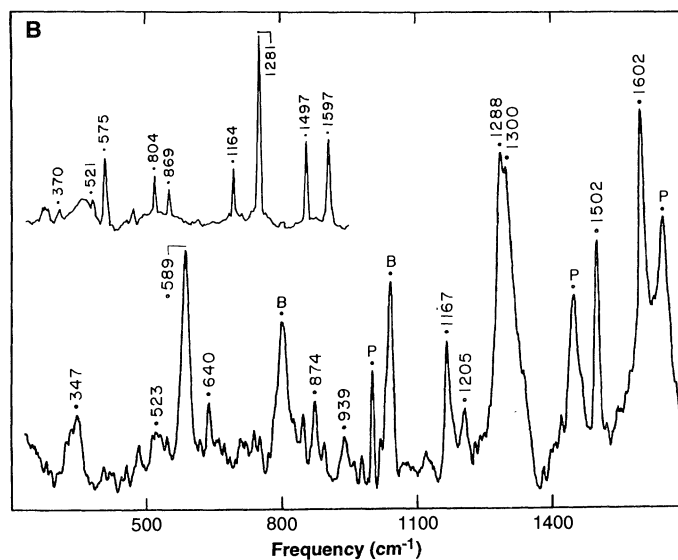


Fig. 3. (A) Kinetics of color formation for H-subunit bullfrog red cell ferritin with one Fe atom per subunit. Purple color due to Fe(III)-Tyr (550-nm peak) (---); amber color of multinuclear Fe(III)-oxo species (absorbance at 420 nm) (—). An arrow indicates the time of admission of air. An anaerobic sample of H-subunit ferritin (1 mM in subunits) in MOPS buffer, pH = 7.0, containing 0.45 M Cl⁻, was incubated with 1 mM Fe(II) for 15 min under argon, then exposed to a flow of moistened air at 25°C. Ultraviolet-visible difference spectra were measured at 30-s intervals with a Hewlett-Packard HP 8452A diode array spectrophotometer interfaced with a microcomputer. We zeroed the spectrometer by using the sample just before the addition of the Fe(II). The results are representative of five independent experiments. **(Inset)** Ultraviolet-visible difference spectrum of the H subunit-specific Fe-protein (purple) complex. The spectrum was measured for the sample in (A) 6 min after the admission of air. **(B)** Resonance Raman spectrum of the H subunit-specific Fe-protein complex. Protein modes at 1002, 1450, and 1650 cm⁻¹ are marked P, and buffer modes at 810 and 1044 cm⁻¹ are marked B. An anaerobic sample



of 0.17 mM H-subunit apoferritin (4 mM in subunits) in MOPS buffer, pH = 7.0, containing 0.45 M Cl⁻, was incubated with 4 mM Fe(II) for 1 hour under argon. After the sample was exposed to air for 5 min, several aliquots were removed and transferred to argon-purged capillary tubes, which were frozen in liquid nitrogen and flame-sealed. The Raman sample was thawed, maintained at ≈10°C in a metal cold-finger submerged in an ice bath (30), and subjected to 572-nm (50-mW) excitation from a Coherent 599-01 dye (rhodamine 6G) and Innova 90-6 argon laser pair. The spectrum was measured at a 90° scattering geometry with a Dilor Z-24 Raman spectrometer at a resolution of 6 cm⁻¹ and a total exposure time of 2.5 hours and was subjected to a 13-point smoothing. The results are representative of two samples. **(Inset)** Resonance Raman spectrum of Fe(III)-Tyr in purple acid phosphatase obtained with 514-nm excitation. [Reprinted in part from (31), with permission © American Chemical Society]

first site at which Fe binds on the path to oxidation and mineralization. The heterogeneity of the Fe(III)-tyrosinate $\nu_{\text{V-O}}$ Raman modes could arise from different conformers involving Fe(III)-Tyr²⁵. Alternatively, Tyr²⁵ and another nearby Tyr, such as Tyr²⁸ or Tyr³⁰, might both be involved. Multiple $\nu_{\text{C-O}}$ Raman modes have been observed for protocatechuate 3,4-dioxygenase, which has two Tyr ligands per Fe (15, 16). Finally, an additional Fe(III)-Tyr moiety could cause heterogeneity in the Raman spectrum. Such a site could be Tyr¹³³, which, although conserved in all known vertebrate H-subunit ferritins, is also in mouse L (17) and bullfrog red cell L (9) ferritin. It is close to the Tb³⁺-binding "ferroxidase" site in human H-subunit ferritin (14). Involvement of Tyr¹³³ would require an environment unique to the H subunit because the L subunit does not form detectable amounts of the Fe(III)-Tyr complex (18).

The Fe(III)-Tyr complex appears to be a transient precursor of polynuclear cluster formation. Such a notion is supported by the observation that smaller numbers of Fe atoms per ferritin formed Fe(III)-Tyr complexes with greater stability and a larger fraction of monomeric Fe(III) (19). On the basis of quantitation of the $g' = 4.3$ signal in the electron paramagnetic resonance (EPR) spectrum (19), ferritin with 24 Fe atoms per molecule contained $20 \pm 4\%$ monomeric Fe(III). If all the monomeric Fe was present as Fe(III)-Tyr, the molar extinction coefficient, $\epsilon_{550 \text{ nm}}$, is $1800 \pm 400 \text{ M}^{-1}$ on a per-metal basis, which is within the range found for Fe(III)-Tyr proteins (1200 to 4000 M^{-1}) (20). Finally, x-ray absorption near-edge structure (XANES) spectroscopy (19) showed that all of the Fe was present as Fe(III); therefore, the EPR-silent Fe is likely to be multimeric Fe(III).

Tyrosine as a ligand for Fe in ferritin has been little discussed. Previously, attention had been focused either on Glu residues conserved in all subunit types or on the Glu⁵⁸ and His⁶¹ residues, which have been considered to be H-subunit specific, at least in mammals (2, 7, 8, 10). The presence of the Glu⁵⁸ and His⁶¹ residues in bullfrog red cell L-subunit ferritin demonstrates their lack of subunit specificity. Clearly, these residues alone are not sufficient to confer a rapid rate of mineralization on the protein (Figs. 1B and 2). The H subunit-specific Fe(III)-Tyr species (Fig. 3A) may be a key to understanding the differences in the mineralization rate of ferritin protein formed from H or L subunits.

REFERENCES AND NOTES

- 1 E. C. Theil, *Adv. Enzymol. Relat. Areas Mol. Biol.* **63**, 421 (1990).
- 2 P. M. Harrison and T. H. Lilley, in *Iron Carriers and Iron Proteins*, T. M. Loehr, Ed. (VCH, New York, 1989), pp. 123–238.

- 3 M. J. Grossman *et al.*, *Proc. Natl. Acad. Sci. U.S.A.* **89**, 2419 (1992).
- 4 M. Ragland *et al.*, *J. Biol. Chem.* **265**, 18339 (1990).
- 5 C. Y. Yang *et al.*, *Biochemistry* **26**, 497 (1987).
- 6 E. Bauminger, P. M. Harrison, I. Nowik, A. Treffrey, *ibid.* **28**, 5486 (1989).
- 7 P. M. Hanna, N. D. Chasteen, G. A. Rottman, P. Aisen, *ibid.* **30**, 9210 (1991).
- 8 D. M. Lawson *et al.*, *Nature* **349**, 541 (1991).
- 9 L. F. Dickey *et al.*, *J. Biol. Chem.* **262**, 7901 (1987).
- 10 V. J. Wade *et al.*, *J. Mol. Biol.* **221**, 1443 (1991).
- 11 M. J. Yablonski and E. C. Theil, *Biochemistry* **31**, 9680 (1992).
- 12 L. Que, Jr., in (2), pp. 457–524.
- 13 ———, in *Biological Applications of Raman Spectroscopy*, T. G. Spiro, Ed. (Wiley, New York, 1988), vol. 3, pp. 491–521.
- 14 R. W. Rice, G. C. Ford, J. L. White, J. M. A. Smith, P. M. Harrison, *Adv. Inorg. Biochem.* **5**, 39 (1983).
- 15 D. H. Ohlendorf, J. D. Lipscomb, P. C. Weber, *Nature* **336**, 403 (1988).
- 16 L. Que, Jr., and R. M. Epstein, *Biochemistry* **20**, 2545 (1981).
- 17 C. Beaumont *et al.*, *J. Biol. Chem.* **264**, 7498 (1989).
- 18 The purple Fe(III)-Tyr complex was not observed in the L subunit, even though Tyr¹³³ is present. However, it could have formed in amounts undetectable if its concentration was low as a result of rapid conversion to Fe(III) bound to other residues. Alternatively, Fe(III)-Tyr may not form in L-subunit ferritin, which may be related to the low rate of mineralization (Fig. 1B).
- 19 After maximum formation of the 550-nm absorbance, samples were rapidly transferred to Ar-purged quartz EPR tubes and frozen in liquid nitrogen. We measured x-band EPR spectra with a JEOL-JES RE-1X spectrometer equipped with a TE011 cylindrical cavity operated at 100 K, 1-mW microwave power, 9.20-GHz microwave frequency, and 1-mT modulation. The fraction of monomeric Fe(III) in each sample was determined by double integration of the $g' = 4.3$ signal from 110 to 220 mT, relative to a 1 mM Fe nitritotriacetic acid standard in 50% glycerin, pH = 4.5. Spectra from XANES (x-ray absorption near edge structure) spectroscopy were measured at 77 K in collaboration with D. E. Sayers on beamline X11-A at the National Synchrotron Light Source. We quantified Fe(II) and Fe(III) by fitting with linear combinations of model compounds as in (21).
- 20 L. Que, Jr., *Coord. Chem. Rev.* **50**, 73 (1983).
- 21 M.-S. Joo, G. Tourillon, D. E. Sayers, E. C. Theil, *Biol. Met.* **3**, 171 (1990).
- 22 F. W. Studier, A. H. Rosenberg, J. J. Dunn, J. S. Dubendorff, *Methods Enzymol.* **185**, 60 (1990).
- 23 M. Heusterspreute and R. R. Crichton, *FEBS Lett.* **129**, 322 (1981).
- 24 D. Boyd *et al.*, *J. Biol. Chem.* **260**, 11755 (1985).
- 25 E. A. Leibold and H. N. Munro, *ibid.* **262**, 7335 (1987).
- 26 S. Daniels-McQueen *et al.*, *Nucleic Acids Res.* **16**, 7741 (1988).
- 27 M. J. Murray, K. White, H. N. Munro, *Proc. Natl. Acad. Sci. U.S.A.* **84**, 7438 (1987).
- 28 P. W. Stevens, J. B. Dodgson, J. D. Engel, *Mol. Cell. Biol.* **7**, 1751 (1987).
- 29 Abbreviations for the amino acid residues are: A, Ala; C, Cys; D, Asp; E, Glu; F, Phe; G, Gly; H, His; I, Ile; K, Lys; L, Leu; M, Met; N, Asn; P, Pro; Q, Gln; R, Arg; S, Ser; T, Thr; V, Val; W, Trp; and Y, Tyr.
- 30 T. M. Loehr and J. Sanders-Loehr, *Methods Enzymol.*, in press.
- 31 B. A. Averill *et al.*, *J. Am. Chem. Soc.* **109**, 3760 (1987).
- 32 J. W. Pyrz, A. L. Roe, L. J. Stern, L. Que, Jr., *ibid.* **107**, 614 (1985).
- 33 We thank D. Stout and S. Sreedharan for engineering the ferritin proteins, M. Forbes for use of the JEOL-JES RE-1X EPR spectrometer, and P. Aisen for helpful discussions on spin quantitation. Support by NIH grants DK-20251 (G.S.W. and E.C.T.) and GM-18865 (J.S.-L.).

7 August 1992, accepted 9 November 1992

Molecular Positional Order in Langmuir-Blodgett Films by Atomic Force Microscopy

L. Bourdieu, O. Ronsin, D. Chatenay

Langmuir-Blodgett films of barium arachidate have been studied on both macroscopic and microscopic scales by atomic force microscopy. As prepared, the films exhibit a disordered hexagonal structure; molecularly resolved images in direct space establish a connection between the extent of the positional order and the presence of defects such as dislocations. Upon heating, the films reorganize into a more condensed state with a centered rectangular crystallographic arrangement; in this new state the films exhibit long-range positional order and unusual structural features, such as a height modulation of the arachidic acid molecules.

Langmuir-Blodgett (LB) films (1) have attracted much attention because of their potential use in molecular electronics (2), integrated optics (3), and the development of biological sensors (4); in addition to these practical applications, LB films are also used as model systems for certain aspects of two-dimensional (2-D) physics such as the description of 2-D solids and the

existence of hexatic phases. For practical applications, one must consider the structure and thermal behavior of the films on both macroscopic and microscopic scales; from a fundamental point of view it has not yet been possible to establish a link between the extent of the positional order in these systems and the presence of defects at the molecular level. For these investigations, atomic force microscopy (AFM) has recently been shown to be a powerful tool (5–9). In contrast to other techniques such as x-ray (10–12) and electron (13–15) diffrac-

Institut Curie, Section de Physique et Chimie, Laboratoire de Physico-Chimie des Surfaces et Interfaces, Unité Associée CNRS 1379, 11 rue Pierre et Marie Curie, 75005 Paris, France.